

Corrosion Behavior of $\text{Cu}_{60}\text{Zr}_{30}\text{Ti}_{10}$ Metallic Glass in the Cl^- Containing Solution

Wei-Ke An¹, An-hui Cai^{1,2}, Xiang Xiong², Yong Liu², Yun Luo¹, Tie-lin Li¹, Xiao-Song Li¹

¹College of Mechanical Engineering, Hunan Institute of Science and Technology, Yueyang, China; ²State Key Laboratory of Powder Metallurgy, Central South University, Changsha, China.
Email: anweike12@163.com

Received December 24th, 2010; revised March 10th, 2011; accepted April 6th, 2011.

ABSTRACT

$\text{Cu}_{60}\text{Zr}_{30}\text{Ti}_{10}$ (at%) ribbon was prepared by melt spinning. Its glassy structure was confirmed by X-ray diffraction (XRD). Its corrosion behavior in HCl and NaCl solutions was investigated by electrochemical polarization measurement. The surfaces before and after corrosion were observed with scanning electron microscope (SEM) and analysis was performed using electron dispersive spectroscopy (EDS). The results show that the decrease of current density is due to the formation of a mixture of simple oxides or complex oxidic compounds. In both cases, the corrosion potential decreases with increasing chloride concentration. The passive film forms easier in HCl than in NaCl. In addition, the higher is the chloride concentration, the easier is the passivation.

Keywords: Metallic Glass, Corrosion Behavior, Chloride Media

1. Introduction

Metallic glasses have acquired significant attention from the scientific and technological viewpoints. They usually show high strength, a large elastic strain limit, and excellent wear and corrosion resistances, along with other remarkable engineering properties [1]. A number of metallic glasses have been used in practical applications. For example, Pd-Cu-Ni-P metallic glasses were used as die materials while Zr-based metallic glasses were used for sporting equipments. In addition, the metallic glasses have also been proposed for some biomedical applications [2,3]. For example, it can be used for making bone fracture fixation and hip arthroplasty components where a low modulus comparable to bone is critical to avoid stress shielding. Furthermore, the superior strength would permit a smaller, less intrusive device that would be capable of withstanding the large forces generated within the skeletal system of the human body [2]. However, the applications of the metallic glasses require high chemical stability in various environments in order to ensure its lifetime. Without high corrosion resistance in the service environments, their favorable mechanical properties cannot be fully exploited. Up to now, a number of corrosion studies have already been reported for metallic glasses in different corrosive media [4-11]. In order to expand the fields of applications of the metallic

glasses, the development of new metallic glasses with better mechanical properties and higher corrosion resistance for lower cost is desirable. Compared with Zr- and Pd-based metallic glasses, Cu-based metallic glasses exhibit even higher mechanical properties and lower cost [12,13]. The Cu-Zr-Ti ternary system is a typical glass forming system first explored by Inoue's group [14]. The maximum size for glass formation in this system can be up to 5 mm [13]. However, it is found that the corrosion resistance of Cu-based metallic glasses is low in acidic solutions, especially when chloride ions are present [15]. In order to apply this type of metallic glasses as engineering materials, the corrosion resistance and the effect of additional elements on Cu-based metallic glasses, such as Cu-Zr [10,11], Cu-Zr-Ti-Nb [16], Cu-Hf-Ti-(Mo, Ta and Nb) [17], Cu-Zr-Ti-Ni-(Nb, Cr, Mo and W) [18-20], Cu-Zr-Ti-(Mo, Ta and Nb) [15], and Cu-Zr-Al-Y [21] have been carried out. Many researches have shown that they are strongly susceptible to chloride-induced pitting corrosion. For example, Zender, *et al.* [22] investigated the corrosion performances of $\text{Cu}_{46}\text{Zr}_{42}\text{Al}_7\text{Y}_5$ and $\text{Zr}_{58.5}\text{Cu}_{15.6}\text{Ni}_{12.8}\text{Al}_{10.3}\text{Nb}_{2.8}$ bulk metallic glasses in 0.001 - 0.1 M HCl aqueous solutions. They found that in both cases the corrosion potential changed to more positive potentials and the corrosion current increased with increasing chloride concentration. However, the pitting potential

decreased and the usable passive region became smaller with increasing chloride concentration. Recently, Gostin, *et al.* [5] have investigated the corrosion behavior of $(\text{Fe}_{44.3}\text{Cr}_5\text{Co}_5\text{Mo}_{12.8}\text{Mn}_{11.2}\text{C}_{15.8}\text{B}_{5.9})_{98.5}\text{Y}_{1.5}$ bulk metallic glass in 0.01 - 0.6 M NaCl aqueous solutions. They found that the corrosion potential was larger in 0.01 M NaCl aqueous solution than in 0.1 and 0.6 M NaCl aqueous solutions. Thus, it is of interest to investigate the influence of the Cl^- concentration on the corrosion property of metallic glasses. In present work, the corrosion behavior of $\text{Cu}_{60}\text{Zr}_{30}\text{Ti}_{10}$ metallic glass is investigated in HCl and NaCl aqueous solutions with different Cl^- concentration.

2. Experimental

$\text{Cu}_{60}\text{Zr}_{30}\text{Ti}_{10}$ (at%) ternary alloy ingots were prepared from the mixture of pure metals by arc melting in an argon atmosphere. Ribbon samples with a thickness of 50 μm and a width of 1.3 mm were prepared by melt spinning at the wheel speed of 30 ms^{-1} . The glassy structure was confirmed by X-ray diffraction (XRD) using Cu K_α radiation.

Corrosion behavior of the glassy alloys was investigated by electrochemical polarization measurement. Prior to electrochemical measurements, the specimens were degreased in acetone, washed in distilled water and dried in air. Electrolytes were NaCl and HCl aqueous solutions whose concentrations were 0.005, 0.01, 0.5, and 1 M, respectively, which were prepared from reagent grade chemicals and deionized water. Electrochemical measurements were conducted using a three-electrode cell with a platinum foil as a counter electrode. The reference electrode was a standard saturated calomel electrode (SCE). All potentials given in this article are referred to the SCE electrode. Potentiodynamic polarization curves were measured with an IM6ex instrument at a potential sweep rate of 0.05 $\text{mV}\cdot\text{s}^{-1}$. The cell was open to air at room temperature and measurement started after the immersion of the samples for 20 min so that the open-circuit potentials of the samples became almost stable. The working electrode was exposed only to an area of 0.04 - 0.08 cm^2 while the rest of the specimen was embedded in a thermoplastic resin to provide electrical isolation. The surfaces of before and after corrosion were observed with an SIRION scanning electron microscope (SEM) and analysis was performed using electron dispersive spectroscopy (EDS).

3. Results

The glassy structure of $\text{Cu}_{60}\text{Zr}_{30}\text{Ti}_{10}$ alloy was confirmed by XRD, the result of which is shown in **Figure 1**. The diffraction pattern exhibits the characteristic broad peak for a glassy structure without any distinct

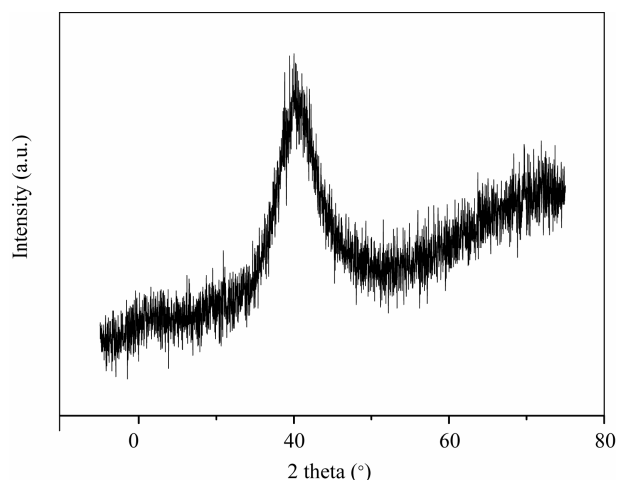


Figure 1. X-ray diffraction pattern for $\text{Cu}_{60}\text{Zr}_{30}\text{Ti}_{10}$ glassy alloy.

crystalline peaks within the sensitivity limit of XRD measurement, indicating the amorphous state of the melt-spun $\text{Cu}_{60}\text{Zr}_{30}\text{Ti}_{10}$ ribbon.

The corrosion behavior of the $\text{Cu}_{60}\text{Zr}_{30}\text{Ti}_{10}$ glassy alloy was examined by potentiodynamic polarization measurement. To ensure reproducibility, at least three measurements were run for each specimen. **Figure 2** shows the anodic and cathodic polarization curves in NaCl and HCl aqueous solutions open to air at room temperature, respectively. As shown in **Figures 2(a)** and **(b)**, the anodic current density increases rapidly without the presence of any passive region when the Cl^- concentration is less than 0.5 M. This indicates that the glassy alloy undertakes strong active dissolution upon anodic polarization and accordingly has a poor corrosion resistance in less than 0.5 M Cl^- solutions. However, the passive procedure starts out in more than 0.5 M Cl^- solutions. The passive potentials are 0.57 V vs SCE in 0.5 M HCl, 0.52 V vs SCE in 1 M HCl, 0.66 V vs SCE in 0.5 M NaCl, and 0.52 V vs SCE in 1 M NaCl, respectively. In addition, the large passive current density up to 0.01 Am^{-2} indicates the pseudopassive behavior. Comparing with **Figure 2(a)** and **Figure 2(b)**, the passive potentials in 1 M HCl and 1 M NaCl are hardly the same, indicating the same passive ability of this glassy alloy in two solutions. However, the passive potential is larger in 0.5 M Cl^- solution than in 1 M Cl^- solution, indicating that the passive procedure easily sets out under higher Cl^- concentration. In addition, the passive potential is larger in 0.5 M NaCl than in 0.5 M HCl, indicating that the passive procedure happens easier in 0.5 M HCl than in 0.5 M NaCl.

On the other hand, the values of the corrosion current density i_{corr} were determined by graphical extrapolation from the polarization curves. The intersection point of

the vertical line corresponding to the corrosion potential E_{corr} , with the tangents on the anodic and cathodic branches was determined. The E_{corr} and i_{corr} values in all solutions are listed in **Table 1**. The relationship between the Cl^- concentration and E_{corr} is plotted in **Figure 3**. It is clearly observed that the corrosion potential decreases with increasing Cl^- concentration in both HCl and NaCl. It indicates that the stability of the metallic glass decreases with increasing Cl^- concentration at thermodynamic point of view. The relationship between the Cl^- concentration and i_{corr} is plotted in **Figure 4**. The corrosion current density in HCl solution slightly increases when the Cl^- concentration is less than 0.1 M, and then decreases with increasing Cl^- concentration. It indicates that the general corrosion decreases when the HCl concentration exceeds 0.1 M. The corrosion current density sharply decreases with increasing NaCl concentration, and then maintains a low value when the NaCl concentration exceeds 0.1 M.

In addition, the corrosion rate was calculated by Faraday's law [23]:

$$\text{Corrosion rate (cm/y)} = \frac{3.16 \times 10^7 \times i_{\text{corr}} \times M}{z \times F \times \rho}, \quad (1)$$

where i_{corr} is the corrosion current density ($\text{A}\cdot\text{cm}^{-2}$), M is the molar mass of the metal ($\text{g}\cdot\text{mol}^{-1}$), z is number of electrons transferred per metal atom, F is the Faraday's constant, and ρ is the density of the metal ($\text{g}\cdot\text{cm}^{-3}$). The corrosion rate values in all solutions are listed in **Table 1**. The relationship between the corrosion rate and the Cl^- concentration is plotted in **Figure 5**. As shown in **Figure 5**, the corrosion rate increases when the HCl concentration is less than 0.1 M, and then decreases with increasing Cl^- concentration. It indicates that the corrosion resistance increases when the HCl concentration exceeds 0.1 M. However, the corrosion rate decreases with increasing NaCl concentration, and then maintains a low value when the NaCl concentration exceeds 0.1 M.

Furthermore, SEM was employed to investigate the morphologies of the samples after polarization tests. **Figure 6** and **Figure 7** show the SEM micrographs of the surfaces corroded in HCl and NaCl solutions, respectively. As shown in **Figures 6(a)-(c)**, the pits can be clearly observed on the surfaces in less than 0.5 M HCl solutions, indicating the occurrence of the pitting in less than 0.5 M HCl solutions. However, the pits disappear and the cracked passive film due to the heavy attack of corrosion can be observed in 1 M HCl, as shown in **Figure 6(d)**. As shown in **Figure 6(a)** and **Figure 6(b)**, the number and depth of the pits increase with increasing chloride concentration, indicating the decrease of the corrosion resistance. However, the number of the pits obviously decreases and the passive film can be observed

Table 1. The corrosion potential E_{corr} , corrosion current density i_{corr} , and corrosion rate of $\text{Cu}_{60}\text{Zr}_{30}\text{Ti}_{10}$ glassy alloy.

Type of solution	Concentration M	E_{corr} mV vs SCE	i_{corr} $\text{A}\cdot\text{m}^{-2}$	Corrosion rate cm/y
HCl	0.005	12.79	2.19	0.34
	0.01	2.30	2.39	0.37
	0.5	-59.94	1.04	0.16
	1	-76.91	0.48	0.08
NaCl	0.005	23.45	2.70	0.42
	0.01	3.89	0.33	0.05
	0.5	-63.07	0.83	0.13
	1	-78.12	0.17	0.03

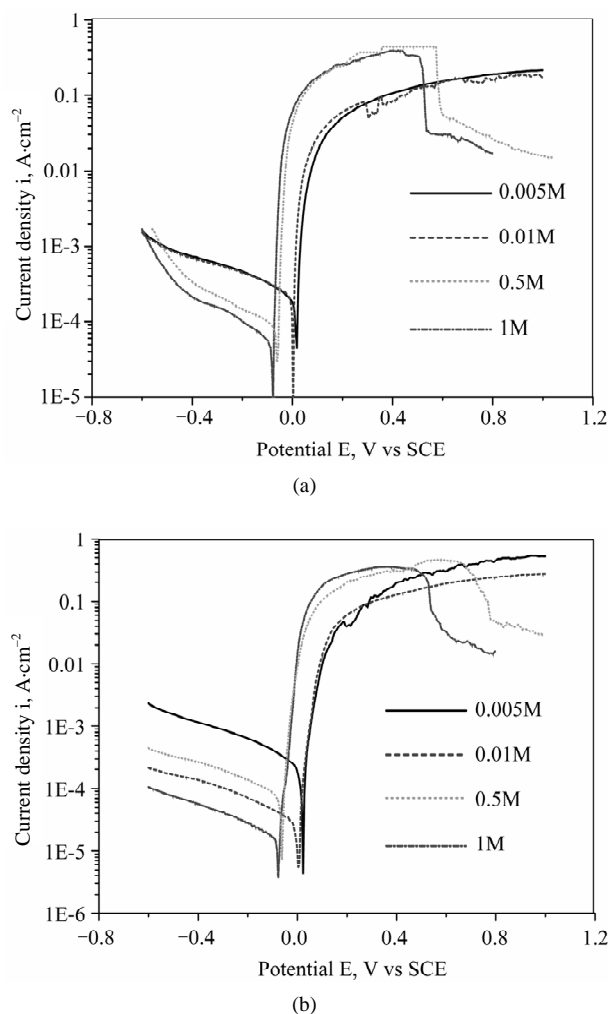


Figure 2. The polarization curves in aqueous solutions containing different Cl^- concentration open to air at room temperature. (a) For HCl; (b) For NaCl.

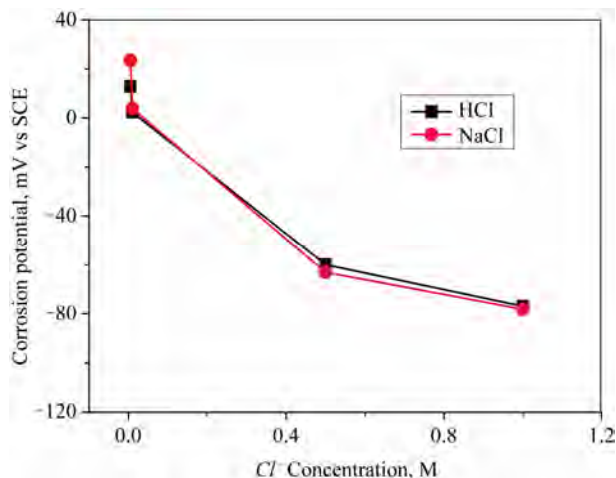


Figure 3. The relationships between the Cl⁻ concentration and corrosion potential E_{corr} .

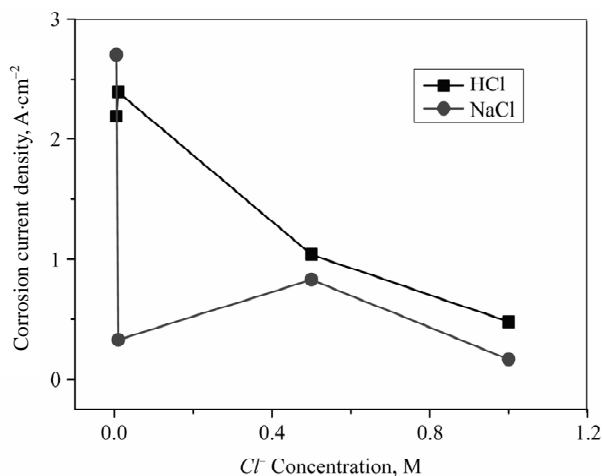


Figure 4. The relationships between the Cl⁻ concentration and corrosion current density i_{corr} .

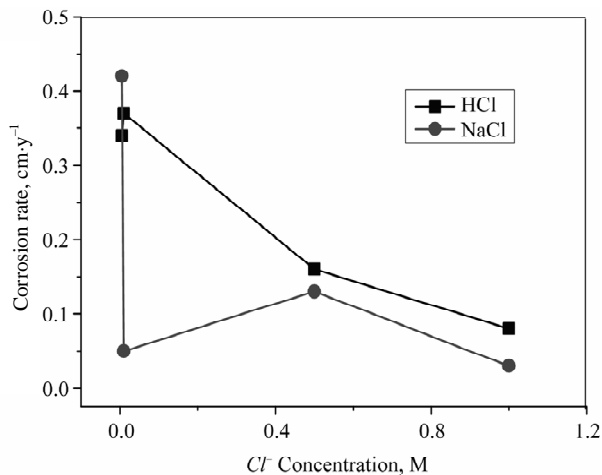


Figure 5. The relationships between the Cl⁻ concentration and the corrosion rate.

(shown in **Figures 6(c)** and **(d)**), indicating the increase of the corrosion resistance. As shown in **Figure 7**, the pits and corrosion products distribute on the surfaces corroded in all NaCl solutions. The size of the pits decreases with increasing chloride concentration, indicating the increase of the corrosion resistance. However, the number of the pits in 0.5 M NaCl increases, which would be a reason for the decrease of the corrosion resistance. In addition, in order to clearly observe the passive film, the enlarged SEM microstructures in 0.5 and 1 M NaCl solutions are shown in **Figure 8**. One can clearly observe from **Figure 8** that the local passive film appears. These SEM results are in coherent with the potentiodynamic polarization measurements.

4. Discussion

As shown in **Figure 6** and **Figure 7**, the pits display on all corroded surfaces except for in 1 M HCl, indicating that the Cu₆₀Zr₃₀Ti₁₀ metallic glass is susceptible to pitting corrosion in chloride media. However, the pitting corrosion doesn't appear in the potentiodynamic polarization curves, as shown in **Figure 2**. The reasons would be as follows. Ideally, metallic glasses are regarded as being physically and chemically homogeneous, free from secondary phases or inclusions which should diminish or prevent the occurrence of galvanic or localized corrosion [24]. However, in practice the presence of defects in cast samples cannot be completely avoided, at least in commercial production [25]. Not surprisingly, several studies show that some metallic glasses have high pitting susceptibility and pits are initiated at the interface between such defects and the surrounding matrix [5, 10, and 26]. The surface morphology of the melt-spun glassy ribbon is illustrated in **Figure 9**. There are three types of regions, including the relatively flat region, the troughs, and the pores. It would be a reason for the pitting corrosion. The other reason would be the selective dissolution of Ti and Zr, and/or simultaneous dissolution of Cu, Ti and Zr [10,27-29].

As shown in **Figure 2**, there is a sharply increase of current density in polarization curve when the chloride concentration exceeds 0.5 M. It is generally thought of the formation of a CuCl film on the surface in chloride media [10, 30 and 31]. In order to further investigate the composition of the passive film, the EDS analysis was performed on the passive films in 1 M HCl and 1 M NaCl. The results are shown in **Table 2**. It is clearly from **Table 2** that the compositions for the passive film consist of O, Zr, Ti, and Cu, respectively. It indicates that the passive film is composed of a mixture of simple oxides or complex oxidic compounds of all alloying elements. Earlier corrosion studies of Zr_{69.5}Cu₁₂Ni₁₁Al_{7.5} showed that the formation of an amorphous ZrO₂ layer [32]. Cu

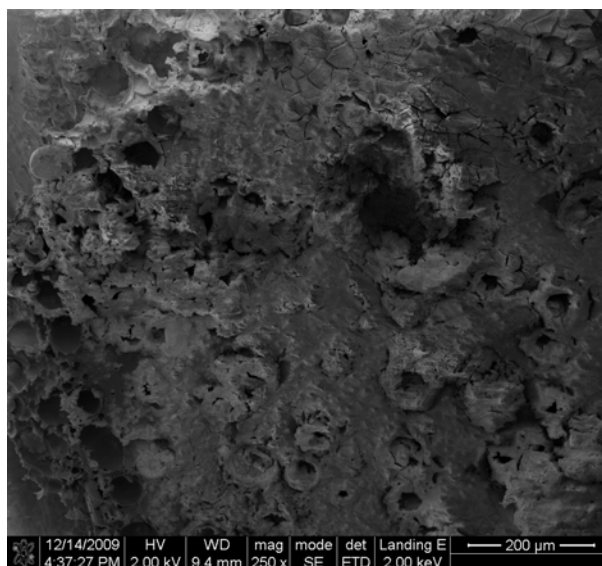
is known to form a protective passive layer of CuO in chloride solution [33]. Corrosion investigations of $\text{Cu}_{50}\text{Zr}_{40}\text{Al}_5\text{Nb}_5$ in 0.5 M NaCl [34] indicated the depletion of Cu in surface film and increases Zr and Nb , leading to the formation of a Zr (Nb)-rich protective surface film. In addition, it is clearly from **Figure 2** that the passive potential decreases with increasing chloride concentration. This would be due to the fact that the pure element displays a lower passive potential in higher chloride concentration. For example, the pure zirconium shows a stable passive state up to $+0.15\text{V}$ in 1.0 mol/L HCl and

$+0.25\text{V}$ in 0.1 mol/L HCl , respectively [10,35]. Thus, the higher is the chloride concentration, the easier is the passivation.

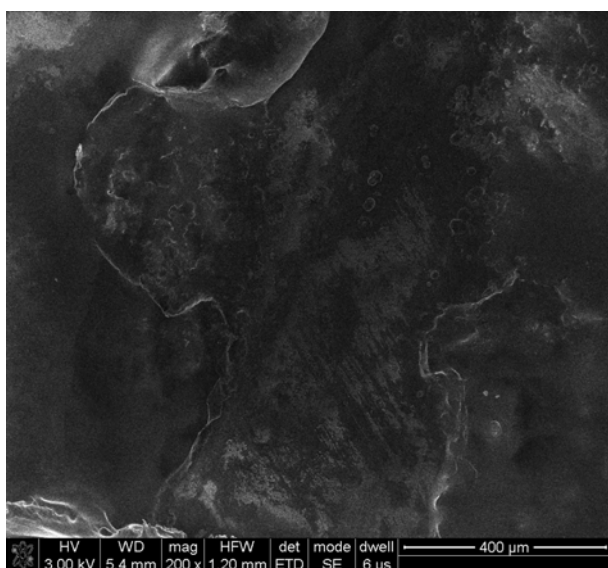
Comparing with **Figure 6(d)** and **Figure 7(d)**, the pit does not appear on the surface corroded in 1 M HCl , while appear on the surface corroded in 1 M NaCl . It would be related with the different distribution of the alloying elements on the surface in HCl and NaCl solutions because the corrosion of metallic glass is strongly influenced by the alloying elements [22]. Asami, *et al.* [15] investigated the concentration of the alloying elements of



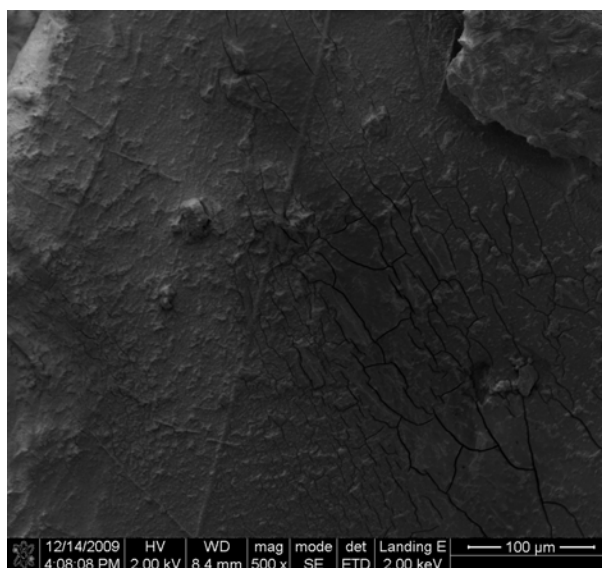
(a)



(b)



(c)



(d)

Figure 6. SEM micrographs of the corroded surfaces in different HCl concentrations, (a) 0.005 M; (b) 0.01 M; (c) 0.5 M; (d) 1 M, respectively.

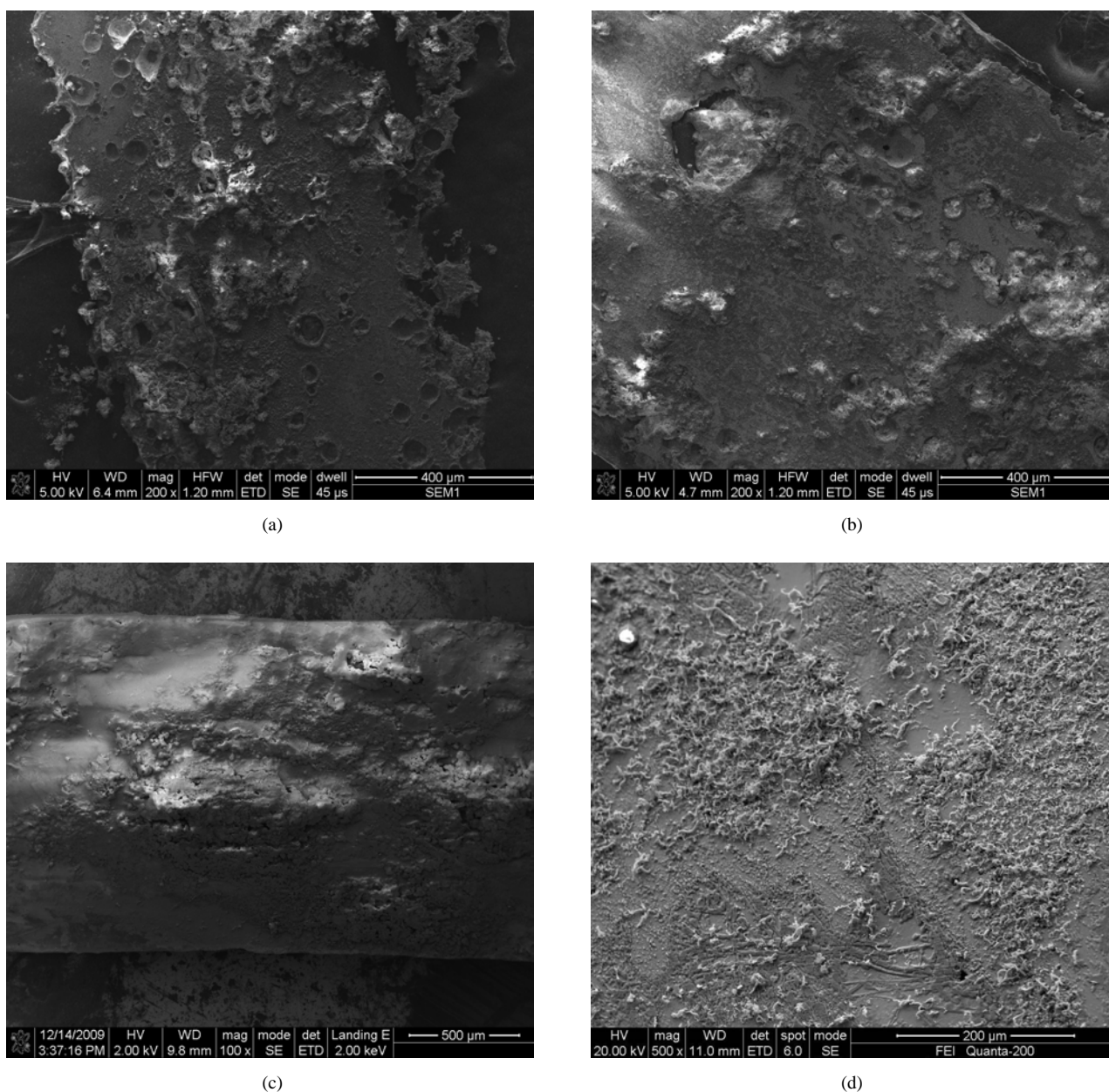


Figure 7. SEM micrographs of the corroded surfaces in different NaCl concentrations, (a) 0.005 M; (b) 0.01 M; (c) 0.5 M; (d) 1 M, respectively.

$\text{Cu}_{60}\text{Zr}_{30}\text{Ti}_{10}$ metallic glass on the surface immersed in 1 N HCl and 3% NaCl, respectively. They found that the cationic fraction of the surface film after immersion in 3% NaCl was almost the same as the alloy composition, but in the surface film formed in 1 N HCl solution, its cationic fraction of Cu was more than the alloy composition. In addition, one can observe from **Table 2** that the content of Cu and Zr + Ti is more in 1 M HCl than in 1 M NaCl. Thus, one can presume that the passive film forms easier and faster in HCl than in NaCl, resulting in the formation of the passive film to prevent the occur-

rence of the pitting corrosion in 1 M HCl. On the other hand, it is well-known that Cu is nobler than Zr and Ti, *i.e.* the standard equilibrium electrode potentials for the Zr/Zr^{4+} , Cu/Cu^{2+} and Ti/Ti^{2+} couples are $-1.529 V_{\text{SHE}}$, $+0.337 V_{\text{SHE}}$ and $-1.628 V_{\text{SHE}}$, respectively. This large electrochemical potential difference between Cu and Zr (Ti) can provide a sufficient potential window for a selective dissolution of Zr (Ti) in Cu-Zr-Ti metallic glass. In addition, the stability of the oxide of the alloying element is different from each other. For example, Zr- and Ti-oxides are more stable chemically and denser struc-

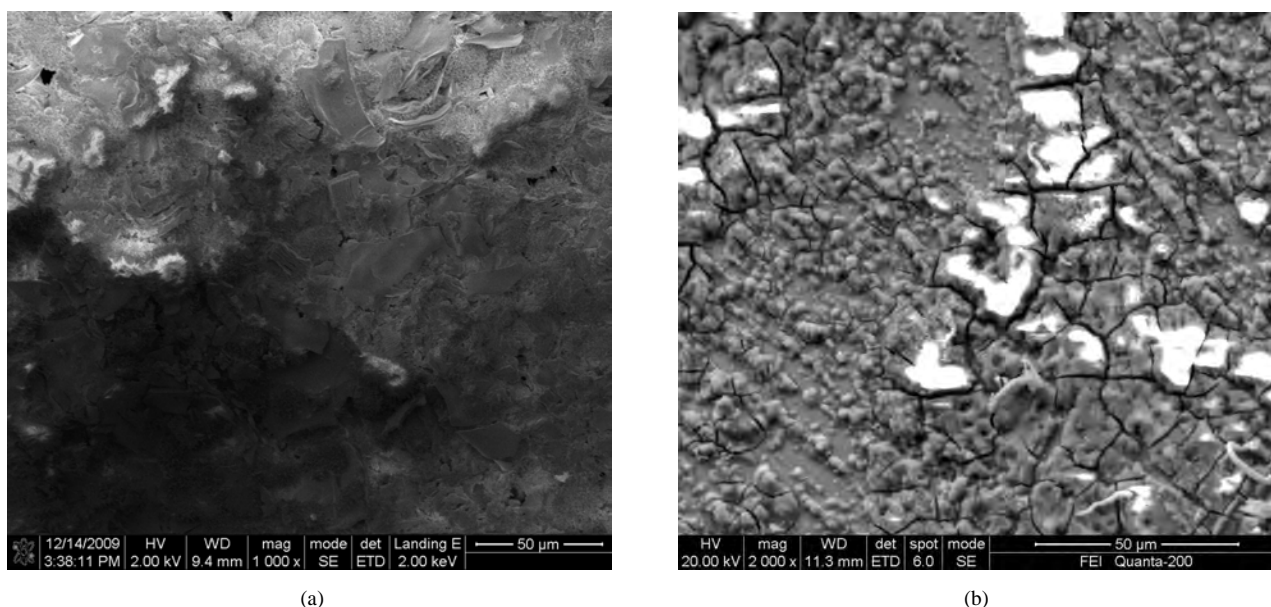


Figure 8. The enlarged SEM micrographs related to the passive films in 0.5 M NaCl (a) and 1 M NaCl (b), respectively.

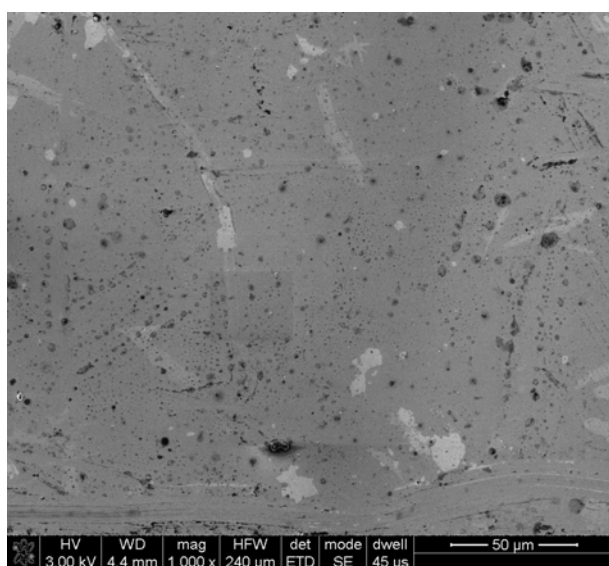


Figure 9. SEM surface morphology of the ribbon before corrosion.

turally than Cu-oxides [20]. These results would result in the different corrosion behavior in HCl and NaCl.

5. Conclusions

The influence of the concentration of HCl and NaCl solutions on corrosion properties of $\text{Cu}_{60}\text{Zr}_{30}\text{Ti}_{10}$ glassy alloy was investigated. The results are as follows.

The corrosion potential decreases with increasing chloride concentration in HCl and NaCl. It indicates that the stability of the metallic glass decreases with increasing chloride concentration at thermodynamic point of

Table 2. Content of alloying elements in passive film in 1 M HCl and 1 M NaCl, respectively.

	O (at%)	Zr (at%)	Ti (at%)	Cu (at%)
1 M HCl	33.63	21.48	3.97	40.91
1 M NaCl	45.32	13.70	7.36	33.62

view.

The corrosion current density and corrosion rate in HCl solution slightly increase, and then decrease when the chloride concentration exceeds 0.1 M. However, the corrosion current density and corrosion rate sharply decrease with increasing NaCl concentration, and then maintain a low value when the NaCl concentration exceeds 0.1 M.

The passive film can form when the chloride concentration exceeds 0.5 M in HCl and NaCl solutions. The passive potentials are 0.57 V vs SCE in 0.5 M HCl, 0.52 V vs SCE in 1 M HCl, 0.66 V vs SCE in 0.5 M NaCl, and 0.52 V vs SCE in 1 M NaCl, respectively. This indicates that the higher is the chloride concentration, the easier is the passivation. The passive film is composed of a mixture of simple oxides or complex oxidic compounds of all alloying elements.

The passive film forms easier in HCl than in NaCl, which is due to the different distribution of the alloying elements on the surface in HCl and NaCl solutions.

6. Acknowledgements

This work was financially supported by the National Natural Science Foundation (Grant No. 50874045),

Postdoctoral Science Foundation of China (Grant Nos. 20080431021 and 200902472), Postdoctoral Science Foundation of Hunan Province (Grant No. 2008RS4021), and Scientific Research Fund of the Hunan Provincial Education Department (Grant No. 10A044).

REFERENCES

- [1] W. H. Wang, C. Dong and C. H. Shek, "Bulk Metallic Glasses," *Materials Science and Engineering: Reports*, Vol. 44, No. 2-3, 2004, pp. 45-89.
[doi:10.1016/j.mser.2004.03.001](https://doi.org/10.1016/j.mser.2004.03.001)
- [2] M. L. Morrison, R. A. Buchanan, R. V. Leon, C. T. Liu, B. A. Green, P. K. Liaw and J. A. Horton, "The Electrochemical Evaluation of a Zr-Based Bulk Metallic Glass in a Phosphate-Buffered Saline Electrolyte," *Journal of Biomedical Materials Research A*, Vol. 74A, No. 3, 2005, pp. 430-438. [doi:10.1002/jbm.a.30361](https://doi.org/10.1002/jbm.a.30361)
- [3] S. Hiromoto, A. P. Tsai, M. Sumita and T. Hanawa, "Effect of Chloride Ion on the Anodic Polarization Behavior of the Zr₆₅Al_{17.5}Ni₁₀Cu_{17.5} Amorphous Alloy in Phosphate Buffered Solution," *Corrosion Science*, Vol. 42, No. 9, 2000, pp. 1651-1660.
- [4] A. P. Wang, X. C. Chang, W. L. Hou and J. Q. Wang, "Corrosion Behavior of Ni-Based Amorphous Alloys and Their Crystalline Counterparts," *Corrosion Science*, Vol. 49, No. 6, 2007, pp. 2628-2635.
[doi:10.1016/j.corsci.2006.12.017](https://doi.org/10.1016/j.corsci.2006.12.017)
- [5] P. F. Gostin, A. Gebert and L. Schultz, "Comparison of the Corrosion of Bulk Amorphous Steel with Conventional Steel," *Corrosion Science*, Vol. 52, No. 1, 2010, pp. 273-281. [doi:10.1016/j.corsci.2009.09.016](https://doi.org/10.1016/j.corsci.2009.09.016)
- [6] Z. M. Zhang, J. Zhang, X. C. Chang, W. L. Hou and J. Q. Wang, "Structure Inhibited Pit Initiation in a Ni-Nb Metallic Glass," *Corrosion Science*, Vol. 52, No. 4, 2010, pp. 1342-1350.
- [7] R. V. S. Rao, U. Wolff, S. Baunack, J. Eckert and A. Gebert, "Corrosion Behaviour of the Amorphous Mg₆₅Y₁₀Cu₁₅Ag₁₀ Alloy," *Corrosion Science*, Vol. 45, No. 4, 2003, pp. 817-832.
[doi:10.1016/S0010-938X\(02\)00131-2](https://doi.org/10.1016/S0010-938X(02)00131-2)
- [8] S. J. Pang, T. Zhang, K. Asami and A. Inoue, "Bulk Glassy Fe-Cr-Mo-C-B Alloys with High Corrosion Resistance," *Corrosion Science*, Vol. 44, No. 8, 2002, pp. 1847-1856. [doi:10.1016/S0010-938X\(02\)00002-1](https://doi.org/10.1016/S0010-938X(02)00002-1)
- [9] A. Gebert, P. F. Gostin and L. Schultz, "Effect of surface Finishing of a Zr-Based Bulk Metallic Glass on Its Corrosion Behaviour," *Corrosion Science*, Vol. 52, No. 5, 2010, pp. 1711-1720. [doi:10.1016/j.corsci.2010.01.027](https://doi.org/10.1016/j.corsci.2010.01.027)
- [10] H. B. Lu, Y. Li and F. H. Wang, "Dealloying Behaviour of Cu-20Zr Alloy in Hydrochloric Acid Solution," *Corrosion Science*, Vol. 48, No. 8, 2006, pp. 2106-2119.
[doi:10.1016/j.corsci.2005.08.009](https://doi.org/10.1016/j.corsci.2005.08.009)
- [11] H. B. Lu, L. C. Zhang, A. Gebert and L. Schultz, "Pitting Corrosion of Cu-Zr Metallic Glasses in Hydrochloric Acid Solutions," *Journal of Alloys Compounds*, Vol. 462, No. 1-2, 2008, pp. 60-67.
[doi:10.1016/j.jallcom.2007.08.023](https://doi.org/10.1016/j.jallcom.2007.08.023)
- [12] A. Inoue, "Stabilization of Metallic Supercooled Liquid and Bulk Amorphous Alloys," *Acta Materialia*, Vol. 48, No. 1, 2000, pp. 279-306.
[doi:10.1016/S1359-6454\(99\)00300-6](https://doi.org/10.1016/S1359-6454(99)00300-6)
- [13] A. Inoue, W. Zhang, T. Zhang and K. Kurosaka, "High-Strength Cu-Based Bulk Glassy Alloys in Cu-Zr-Ti and Cu-Hf-Ti Ternary Systems," *Acta Materialia*, Vol. 49, No. 14, 2001, pp. 2645-2652.
[doi:10.1016/S1359-6454\(01\)00181-1](https://doi.org/10.1016/S1359-6454(01)00181-1)
- [14] A. Inoue, W. Zhang, T. Zhang and K. Kurosaka, "Thermal and Mechanical Properties of Cu-Based Cu-Zr-Ti Bulk Glassy Alloys," *Materials Transactions JIM*, Vol. 42, No. 6, 2001, pp. 1149-1151.
[doi:10.2320/matertrans.42.1149](https://doi.org/10.2320/matertrans.42.1149)
- [15] K. Asami, C. Qin, T. Zhang and A. Inoue, "Effect of Additional Elements on the Corrosion Behavior of a Cu-Zr-Ti Bulk Metallic Glass," *Materials Science and Engineering: A*, Vol. 375-377, No. 7, 2004, pp. 235-239.
[doi:10.1016/j.msea.2003.10.034](https://doi.org/10.1016/j.msea.2003.10.034)
- [16] C. Qin, K. Asami, T. Zhang, W. Zhang and A. Inoue, "Corrosion Behavior of Cu-Zr-Ti-Nb Bulk Glassy Alloys," *Materials Transactions JIM*, Vol. 44, No. 4, 2003, pp. 749-753. [doi:10.2320/matertrans.44.749](https://doi.org/10.2320/matertrans.44.749)
- [17] F. R. Niessen, "Cohesion in Metals," Elsevier Science, Amsterdam, 1988.
- [18] T. Yamamoto, C. Qin, T. Zhang, K. Asami and A. Inoue, "Formation, Thermal Stability, Mechanical Properties and Corrosion Resistance of Cu-Zr-Ti-Ni-Nb Bulk Glassy Alloys," *Materials Transactions JIM*, Vol. 44, No. 6, 2003, pp. 1147-1152. [doi:10.2320/matertrans.44.1147](https://doi.org/10.2320/matertrans.44.1147)
- [19] B. Liu and L. Liu, "Improvement of Corrosion Resistance of Cu-Based Bulk Metallic Glasses by the Microalloying of Mo," *Intermetallics*, Vol. 15, No. 5-6, 2007, pp. 679-682. [doi:10.1016/j.intermet.2006.10.039](https://doi.org/10.1016/j.intermet.2006.10.039)
- [20] B. Liu and L. Liu, "The Effect of Microalloying on Thermal Stability and Corrosion Resistance of Cu-Based Bulk Metallic Glasses," *Materials Science and Engineering: A*, Vol. 415, No.1-2, 2006, pp. 286-290.
[doi:10.1016/j.msea.2005.09.099](https://doi.org/10.1016/j.msea.2005.09.099)
- [21] M. K. Tam, S. J. Pang and C. H. Shek, "Corrosion Behavior and Glass-Forming Ability of Cu-Zr-Al-Nb Alloys," *Journal of Non-Crystalline Solids*, Vol. 353, No. 32-40, 2007, pp. 3596-3599.
- [22] D. Zander, B. Heisterkamp and I. Gallino, "Corrosion Resistance of Cu-Zr-Al-Y and Zr-Cu-Ni-Al-Nb Bulk Metallic Glasses," *Journal of Alloys and Compound*, Vol. 434-435, No. 5, 2007, pp. 234-236.
[doi:10.1016/j.jallcom.2006.08.112](https://doi.org/10.1016/j.jallcom.2006.08.112)
- [23] D. A. Jonse, "Principles and Prevention of Corrosion," Printice-Hall, New Jersey, 1996.
- [24] K. Hashimoto, "Chemical Properties," In: F. E. Luborsky Ed., *Amorphous Metallic Alloys*, Butterworth, London, 1983, p. 53.
- [25] Y. H. Liu, G. Wang, R. J. Wang, D. Q. Zhao, M. X. Pan and W. H. Wang, "Super Plastic Bulk Metallic Glasses at

- Room Temperature,” *Science*, Vol. 315, No. 3, 2007, pp. 1385-1388. [doi:10.1126/science.1136726](https://doi.org/10.1126/science.1136726)
- [26] A. Gebert, U. Kuehn, S. Baunack, N. Mattern and L. Schultz, “Pitting Corrosion of Zirconium-Based Bulk Glass-Matrix Composites,” *Materials Science and Engineering: A*, Vol. 415, No. 1, 2006, pp. 242-249. [doi:10.1016/j.msea.2005.09.062](https://doi.org/10.1016/j.msea.2005.09.062)
- [27] G. Kear, B. D. Barker and F. C. Walsh, “Electrochemical Corrosion of Unalloyed Copper in Chloride Media—A Critical Review,” *Corrosion Science*, Vol. 46, No. 1, 2004, pp. 109-135. [doi:10.1016/S0010-938X\(02\)00257-3](https://doi.org/10.1016/S0010-938X(02)00257-3)
- [28] M. Chmielová, J. Seidlerová and Z. Weiss, “X-Ray Diffraction Phase Analysis of Crystalline Copper Corrosion Products after Treatment in Different Chloride Solutions,” *Corrosion Science*, Vol. 45, No. 5, 2003, pp. 883-889. [doi:10.1016/S0010-938X\(02\)00176-2](https://doi.org/10.1016/S0010-938X(02)00176-2)
- [29] A. V. Vvedenskii and S. N. Grushevskaya, “Kinetic Peculiarities of Anodic Dissolution of Copper and Its Gold Alloys Accompanied by the Formation of Insoluble Cu (I) Products,” *Corrosion Science*, Vol. 45, No. 10, 2003, pp. 2391-2413. [doi:10.1016/S0010-938X\(03\)00064-7](https://doi.org/10.1016/S0010-938X(03)00064-7)
- [30] R. S. Copper and J. H. Bartlett, “Convection and Film Instability Copper Anodes in Hydrochloric Acid,” *Journal of the Electrochemical Society*, Vol. 105, No. 3, 1958, pp. 109-116. [doi:10.1149/1.2428773](https://doi.org/10.1149/1.2428773)
- [31] L. Stephenson and J. H. Bartlett, “Anodic Behavior of Copper in HCl,” *Journal of the Electrochemical Society*, Vol. 101, No. 11, 1954, pp. 571-581. [doi:10.1149/1.2781156](https://doi.org/10.1149/1.2781156)
- [32] D. Zander and U. Köster, “Corrosion of Amorphous and Nanocrystalline Zr-Based Alloys,” *Materials Science and Engineering: A*, Vol. 375-377, No. 7, 2004, pp. 53-59. [doi:10.1016/j.msea.2003.10.230](https://doi.org/10.1016/j.msea.2003.10.230)
- [33] E. Kunze, “Korrosion und Korrosionsschutz,” Wiley-VCH, Weinheim, 2001.
- [34] C. Qin, W. Zhang, H. Kimura, K. Asami and A. Inoue, “New Cu-Zr-Al-Nb Bulk Glassy Alloys with High Corrosion Resistance,” *Materials Transactions JIM*, Vol. 45, No. 6, 2004, pp. 1958-1961. [doi:10.2320/matertrans.45.1958](https://doi.org/10.2320/matertrans.45.1958)
- [35] H. Bala and S. Szymura, “Acid Corrosion of Amorphous and Crystalline Cu-Zr Alloys,” *Applied Surface Science*, Vol. 35, No. 1, 1988, pp. 41-51. [doi:10.1016/0169-4332\(88\)90036-0](https://doi.org/10.1016/0169-4332(88)90036-0)